INTERNATIONAL JOURNAL OF HYDROGEN ENERGY 52 (2024) 923–932

Available online at www.sciencedirect.com

ScienceDirect

journal homepage: www.elsevier.com/locate/he

An investigation on coupling fuel cell, wind turbine and PV as green to green system

Ahmad Haddad [a,b], *Hadi Jaber* [c], *Mahmoud Khaled* [a,b], *Rafat Al Afif* [d], *Mohamad Ramadan* [a,b,*]

[a] *School of Engineering, International University of Beirut BIU, Beirut, Lebanon*
[b] *School of Engineering, Lebanese International University LIU, Bekaa, Lebanon*
[c] *Mechanical Engineering Department, Abu Dhabi University, United Arab Emirates*
[d] *Institute for Chemical and Energy Engineering (IVET), University of Natural Resources and Life Sciences, Muthgasse 107, 1190, Vienna, Austria*

HIGHLIGHTS

- The work is performed within the frame of Green to Green (G2G) concept that combines green source to green storage.
- Green sources are PV and Wind Turbine whereas the green storage system is fuel cell.
- The developed model is applied to three different regions in Lebanon in order to find the best configuration.

ARTICLE INFO

Article history:
Received 14 December 2021
Received in revised form
10 May 2022
Accepted 12 June 2022
Available online 31 July 2022

Keywords:
G2G
Green to green
Hydrogen
Fuel cell
Solar
Wind

ABSTRACT

In the recent years Green to Green Energy Systems have gain tremendous interest because they are pollution free systems. In this frame, the present paper aims at investigating a Green to Green system coupling Photovoltaic, Wind and Fuel Cell. Furthermore, an analysis procedure is developed allowing to find the optimal configuration of coupling by assessing the output power in terms of the system parameters. Moreover, a case study on Lebanon is considered where three different regions that are Dahr El-Baidar, Klaiaat Akkar and Rayak Bekaa are studied. Results shows the flexibility and strength of the suggested procedure. Indeed, it has been shown that for Dahr El-Baidar it is suggested to adopt WFC system whereas for Klaiaat Akkar hybrid PVWFC is the optimal solution and PVFC is better for Rayak Bekaa. Furthermore, an economic based optimization is carried out. It was surprisingly found that from an economic standpoint and for a land area larger than 3000 m^2 Rayak Bekaa is the optimal location for WFC hybrid system.

Introduction

In the last decade, environmental issues [1] are attracting widespread interest. As a matter of fact, huge effort is being made to reduce the negative impact of energy production on the environment. Many energy systems have been proposed emphasizing on two aspects that are energy production and energy storage [2]. Renewable energy [3] receives the lion's

* *Corresponding author*. School of Engineering, International University of Beirut BIU, Beirut, Lebanon.
E-mail address: mohamad.ramadan@liu.edu.lb (M. Ramadan).
https://doi.org/10.1016/j.ijhydene.2022.06.107
0360-3199/

share of studies covering all types of sustainable sources such as solar energy (SE) [4], wind energy (WE) and geothermal energy [5]. Energy recovery has also been investigated as an indirect sustainable source. On the other hand, green energy storage has been taking an ample attraction since it is an inescapable part of any energy system. Indeed, there are several energy storage strategies that can be adopted such as supercapacitor and batteries. From an environmental point of view, the star of the moment is fuel cell (FC). Moreover, green energy production and green energy storage can be combined through green to green energy system (G2G) [6]. Typical systems are those coupling FC and WE or FC and SE. In Ref. [7] a coupled wind – fuel cell (WFC) system is studied where the authors propose to recover heat and reuse it for the desorption of hydrogen. Genç et al. [8] perform a parametric study by varying hub heights of wind turbine in the frame of WFC coupling. Other smart systems coupling solar energy, wind energy, and hydrogen have also been investigated [9–11]. In Ref. [12] an investigation on hybrid photovoltaic-wind system is performed with both fuel cell and batteries. An optimization procedure for SWFC is discussed in Ref. [13]. Economic study for SWFC is investigated in Ref. [14]. Case study on turkey of SWFC is shown in Ref. [15]. Advanced coupling involving different types of solar system as well as solar thermal system – wind turbine with fuel cell have also been investigated [16,17]. Selecting criteria for hybrid renewable energy systems for residential application in Lagos Nigeria is studied in Ref. [18]. The authors studied different configurations of coupling. They conclude that depending on the considered criteria different optimal systems are obtained. If the economic aspect is imposed then the best configuration is PV-battery, whereas the authors mention that if multi-criteria, such as economic, environmental and technical aspects are considered then Photovoltaic-Wind turbine-fuel cell and battery is the optimal coupling configuration. Hybrid system involving wind turbine, solar system, battery and fuel cell has been investigated experimentally [19]. The study reveals the role of the control system in optimizing the energy output. For this purpose, Single Input Fuzzy Logic (SIFL), is used for maximum power point tracking. Optimizing, hybrid systems involving solar system, wind turbine and fuel cell has been also studied using optimization algorithms such as particle swarm optimization technique and Hybrid Firefly and Harmony Search optimization technique [20]. Analysis of hydrogen production using solar energy and solar energy for polymer electrolyte membrane electrolysis (PEMEL) and alkaline electrolysis (AEL) using modeling is presented in Ref. [21]. The authors conclude that 4.33 €/kg is the Cheapest hydrogen production for alkaline electrolysis coupled to onshore wind turbine.

In the frame of this paper a hybrid Photovoltaic-Wind- Fuel Cell (PVWFC) system is proposed. To proceed a modeling of the proposed coupling strategy is performed. The aim is to find the optimal configuration relying on the key-parameters that controls the output. The study is performed for three different region of Lebanon that are Dahr El-Baidar, Klaiaat Akkar and Rayak Bekaa. This paper is organized as follows. Section two presents the analysis procedure. In section three, wind farm modeling and sizing is discussed. Section four is dedicated to present modeling and sizing of PV array. Electrolyzer and fuel cell modeling and sizing are respectively shown in sections five and six. Section seven is devoted for results and finally concluding remarks are presented in the conclusion.

Methods

Green to green (G2G)

The idea behind the concept of green to green energy system (G2G) that was proposed by Ramadan [6], is to promote energy systems that are entirely eco-friendly and does not have any negative environmental impact. In such systems not only the energy sources should be green but the storage system should also be green, that is to say the storage system should also be pollution-free. From an energetic point of view, any system combining a green source and a green storage could be labeled as G2G. Green energy sources include renewable energy sources such as geothermal energy, solar energy, wind energy, hydropower and wave energy. On the other hand, the panel of green storage systems include many technologies such as hydrogen, flywheel, pumped hydro and compressed air. Fig. 1 shows a schematic presentation of potential G2G systems.

Procedure of selection

The procedure of selection followed in this work is illustrated in Fig. 2. First, the data of the average wind speed for the studied location is used to size the Wind Turbine (WT). The WT sizing includes calculation of its rated power and rotor diameter. Second, the number of wind turbines constituting the wind farm is determined according to the land area and the minimum spacing between wind turbines so that wind speed recovers enough before it reaches the next turbine. From the other side, the Photovoltaic Array is sized according to the Direct Normal Insulation (DNI) and the panels' tilt angle in the studied location, as well as the module's and land's areas. The total powers provided by the two systems are compared all over the year. The system that supplies more power is selected. In case the difference between the two powers varies, coupling is recommended.

Wind farm modeling and sizing

This section deals with modeling and sizing of the wind farm based on the land area and the average wind speed of the studied locations. First, the WT size is selected based on its rated power which depends on the maximum operational wind speed at the best site. The wind speed data show that the average speed can reach 9.1 m/s in some regions in Lebanon during periods of high wind. According to this speed, a WT having the characteristics presented in Table 1 is considered.

The profile of the power curve versus wind speed for the selected WT is shown in Fig. 3. Results show that for a velocity up to 9 m/s the profile can be approximated, with minor error, to a power curve having the following form:

$$P_{WT} = 0.0592 \times S^{3.1394} \quad (1)$$

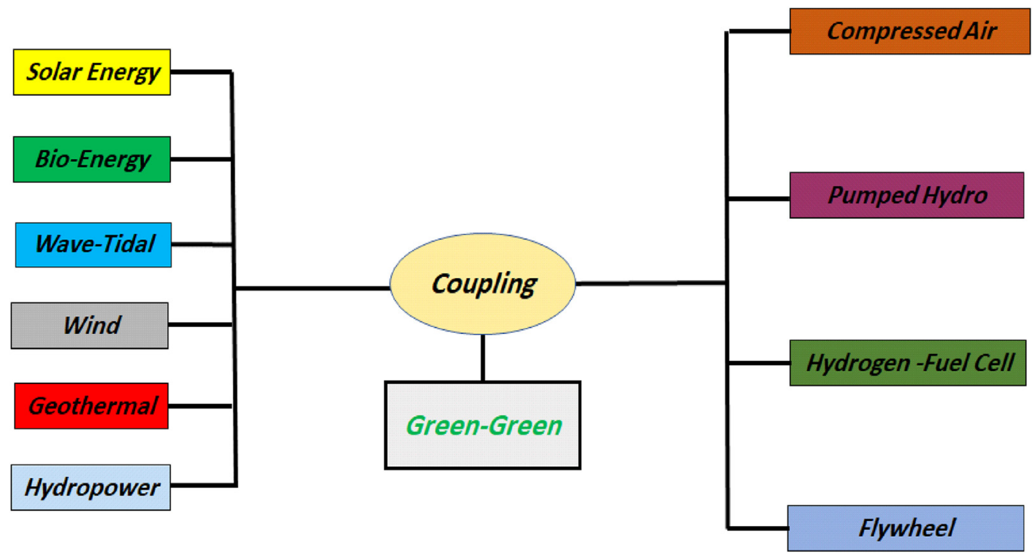

Fig. 1 – Green to Green (G2G) coupling [6]. (For interpretation of the references to color/colour in this figure legend, the reader is referred to the Web version of this article.)

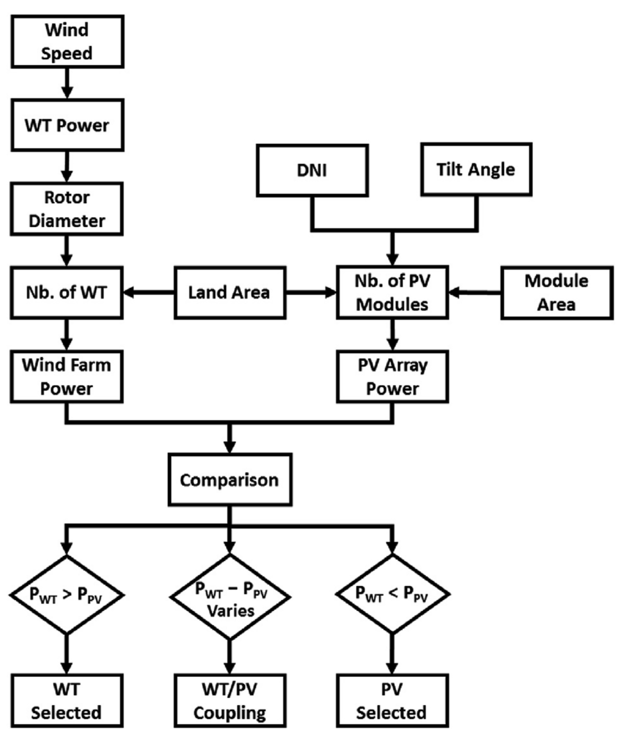

Fig. 2 – Procedure of selection.

Table 1 – Characteristics of the selected WT.	
Rated power	100 kW
Rotor Diameter	25 m
Cut in speed	2.7 m/s
Rated speed	10 m/s
Cut out speed	25 m/s

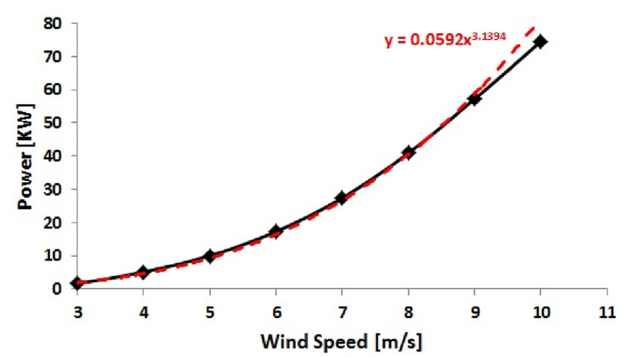

Fig. 3 – WT power profile versus wind speed.

Where, P_{WT} is the WT output power in kW and S is the wind speed in m/s. Equation (1) is used for wind farm power calculation in different locations.

The wind farm size is determined according to the WT rotor's diameter and the available land area. Spacing between wind turbines is a critical factor that should be taken into consideration in sizing wind farms. In fact, a minimum spacing is needed to allow for wind recovery or else the wind power will be lost. Experimental studied reveal that optimum spacing is estimated to be 3 to 5 times rotor diameter between towers and 5 to 9 times between rows as shown in Fig. 4. In this work a rectangular land of 1000 m^2 area is considered. Since the rotor's diameter is 25 m, the minimum spacing between towers in a row is 75 m. Therefore, the wind farm will be composed of 2 wind turbines placed in one row facing the wind direction. Hence, the total wind farm power is:

$$P_{WF} = 2 \times P_{WT} = 0.1184 \times S^{3.1394} \quad (2)$$

PV array modeling and sizing

This section deals with modeling and sizing of the PV array based on the land area, the DNI in the studied location, the tilt

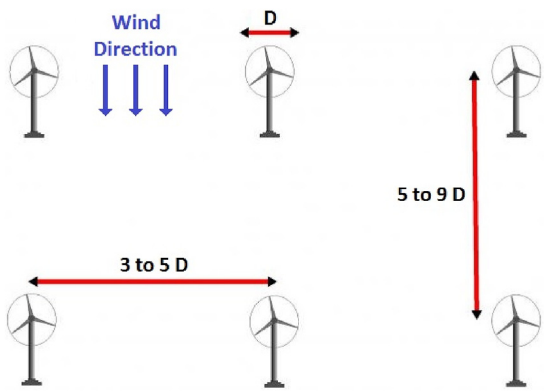

Fig. 4 – Optimum spacing between wind turbines.

angle of the PV module and the DC bus voltage. The PV module used in the array design is a 250W monocrystalline. Its characteristics are given in Table 2.

The PV module is modeled with the equivalent electrical circuit. It mainly behaves as a photocurrent I_{PH} controlled by DNI. A diode is used to represent the PN junction cells from which the module is composed. The voltage and current drops inside the module are respectively represented with a series resistance R_S and a shunt resistance R_{SH}.

Referring to the electrical model, the module's output current is:

$$I_{PV_{Module}} = I_{PH} - I_D - I_{SH} \tag{3}$$

where I_{PH} is module's photocurrent given by:

$$I_{PH} = \left[I_{SC} + K_i(T_M - T_{ref})\right] \times \frac{DNI}{1000} \tag{4}$$

where I_D is module's diode current given by:

$$I_D = I_S\left[exp^{\left(q\times\frac{V_{PV_{Module}}+R_S\ I_{PV_{Module}}}{K\ n\ T_M}\right)} - 1\right] \tag{5}$$

I_{SH} is module's current loss caused by its shunt resistance R_{SH}. It is given by:

$$I_{SH} = \frac{V_{OC}}{R_{SH}} \tag{6}$$

where, K_i is the Temperature coefficient, T_M is Module's temperature, T_{ref} is the Reference temperature (300 K), I_S is Module's saturation current, q is the Quantity of electronic charge, n is Module's ideality factor, K is Boltzmann's constant and $V_{PV_{Module}}$ is Module's operating voltage.

The total output voltage of the PV array is:

Table 2 – Characteristics of the selected PV module.

Rated power P_{max}	250 W
Open circuit voltage V_{OC}	37.8 V
Max. Power point voltage V_{MP}	31.1 V
Short circuit current I_{SC}	8.28 A
Max. Power point current I_{MP}	8.05 A
Dimensions	167.5 × 95.1 cm

$$V_{PV_{Array}} = N_{PV-Series} \times V_{PV_{Module}} \tag{7}$$

where $N_{PV-Series}$ is the Number of series modules in one string.

The total output current of the PV array is:

$$I_{PV_{Array}} = N_{PV-Parallel} \times I_{PV_{Module}} \tag{8}$$

where $N_{PV-Parallel}$ is the number of parallel strings in the array.

The total output power of the PV array is:

$$P_{PV_{Array}} = V_{PV_{Array}} \times I_{PV_{Array}} \tag{9}$$

The PV array size is determined according to the available land area and the panels tilt angle. This latter is a determinant factor in computing the spacing between modules so that to avoid shading and consequently power loss. The optimal tilt angle for the studied locations in Lebanon is $\theta_{optimal} = 30°$. Given the module length (167.5 cm), the minimum spacing distance D between modules is calculated using simple trigonometry as shown in Fig. 5. D is found to be 144 cm.

Based on the shadow distance D, the PV module dimensions and the optimal tilt angle, the maximum number of PV modules that can fit in 1000 m^2 land area is $N_{PV} = 140$ modules. The number of modules in series $N_{PV-Series}$ is the ratio of the array's DC voltage $V_{DC-Array}$ over the module's maximum power point voltage V_{MP} rounded to the next higher integer. To be compatible with the electrolyzer's DC input voltage, we consider $V_{DC-Array} = 150$ V. Therefore,

$$N_{PV-Series} = \left.\frac{V_{DC-Array}}{V_{MP}}\right|_{Rounded} = 5\ Modules \tag{10}$$

Hence, the number of modules in parallel $N_{PV-Parallel}$ is:

$$N_{PV-Parallel} = \frac{N_{PV}}{N_{PV-Series}} = 28\ Modules \tag{11}$$

Electrolyzer modeling and sizing

The fluctuation of wind speed and solar radiations require energy storage to meet the load demand. Storage via battery bank has several disadvantages. In fact, batteries have environmental impacts because of toxic metals which become hazardous waste. Furthermore, their lifetime is limited and harmfully affected with temperature increase. Moreover, they are not suitable for large scale storage because they are heavy, bulky and need to be protected against overcharge/overdischarge and heat. For all these reasons we propose to use hydrogen production as a green storage medium. The stored hydrogen is used to operate the Fuel Cell system which is

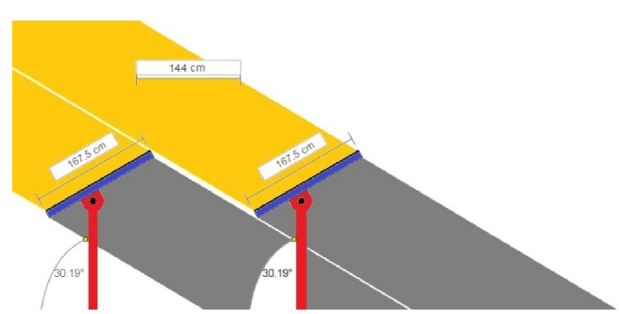

Fig. 5 – Minimum spacing between PV modules.

coupled with the wind farm and the PV array for recovery in case of power shortage. For hydrogen production, an electrolyzer of 60 kW rated power and 150V DC voltage is used. The electrolyzer is sized based on the maximum DC power produced by wind farm/PV array in the studied locations during high wind/radiation times. The hydrogen and oxygen production rates $\dot{m}_{H_2}$ and $\dot{m}_{O_2}$ are:

$$\dot{m}_{H_2} = 2\dot{m}_{O_2} = \frac{n_{cells} \times i_E \times \eta_F}{2\,F} \times 3600 \times \frac{M_{H_2}}{\rho_{H_2}} \tag{12}$$

with n_{cells} is the Number of electrolyzer's cells, F is Faraday's constant, M_{H_2} is molar mass of hydrogen ρ_{H_2} is the density of hydrogen. And η_F is Faraday's efficiency given by:

$$\eta_F = 96.5 \times exp\left(\frac{0.09}{i_E} - \frac{75.5}{i_E^2}\right) \tag{13}$$

where i_E is the Electrolyzer's current given by:

$$i_E = \frac{P_{WF} \times \eta_{Rectifier}}{150\ V}\ (WT\ case) \tag{14}$$

$$i_E = \frac{P_{PV_{Array}}}{150\ V}\ (PV\ case) \tag{15}$$

$\eta_{Rectifier}$: Efficiency of the rectifier used to convert the wind farm's AC power to a DC one.

Fuel cell modeling and sizing

Hydrogen and oxygen produced by the electrolyzer are used to feed the Fuel Cell system for power generation in absence of wind and solar radiation. The fuel cell's output current is function of hydrogen consumption rate as shown in the following equation:

$$i_{FC} = \frac{2\,F \times \dot{m}_{H_2}}{3600} \times \frac{\rho_{H_2}}{M_{H_2}} \tag{16}$$

The output voltage per cell is:

$$V_{cell} = E_{nernst} - V_{act} - V_{ohm} - V_{conc} \tag{17}$$

where E_{nernst} is the open circuit voltage and V_{act} the Activation voltage loss given by:

$$V_{act} = \frac{R_G\,T_{FC}}{2\,F} \times ln\left(\frac{i_{FC}}{i_0}\right) \tag{18}$$

where R_G is Gas constant, T_{FC} is fuel cell temperature and i_0 is Exchange Current and V_{ohm} is Ohmic voltage loss given by:

$$V_{ohm} = (R_A + R_M + R_C) \times i_{FC} \tag{19}$$

where R_A is Anode electrical resistance, R_C is the Cathode electrical resistance, R_M is the Membrane electrical resistance and V_{conc} is the Concentration voltage loss given by:

$$V_{conc} = \frac{R_G\,T_{FC}}{2\,F} \times ln\left(1 - \frac{i_{FC}}{i_{max}}\right) \tag{20}$$

Where, i_{max} is the Limit Current.

The fuel cell's output power is:

$$P_{FC} = V_{FC} \times i_{FC} = N_{cells} \times V_{cell} \times i_{FC} \tag{21}$$

Where, N_{cells} is the Number of stack cells. The fuel cell is sized according to its maximum limit current density, the inverter's input DC voltage as well as its rated power. Based on experimental works, the maximum limit current density j_{max} of the fuel cell is 0.7 A/cm^2 and the minimum guaranteed fuel cell's output voltage is 0.6 V/cell. The results presented in the next section show that the Fuel Cell's rated power is 25 kW during peak wind speed. The DC input voltage of a conventional 220V AC inverter is 48V DC. Hence, the number of cells composing the stack is:

$$N_{cells} = \frac{48\ V}{0.6\ V/cell} = 80\ cells \tag{22}$$

It follows that the fuel cell's maximum current is:

$$i_{FC} = \frac{25000\ W}{48\ V} = 521\ A \tag{23}$$

Therefore, the cell's area is:

$$A_{cell} = \frac{521\ A}{0.7\ A/cm^2} = 744\ cm^2 \tag{24}$$

Results and discussions

In the current work, three locations are studied: Dahr Al-Baidar region located in Mount-Lebanon (Latitude: 33°48′ North – Longitude: 35°46′ East, Elevation: 1555 m), Klaiaat Akkar region located in North-Lebanon (Latitude: 34°35′ North – Longitude: 35°59′ East, Elevation: 23 m) and Rayak region located in Bekaa Valley (Latitude: 33°50′ North – Longitude: 36°1′ East, Elevation: 920 m). Wind speed data for the selected locations are taken from the Lebanese ministry of energy and water. Solar insulation data are taken from the Photovoltaic Geographical Information System (PVGIS) of the European Communities from 2001 to 2012.

Case study of Dahr El-Baidar

Comparison between average wind speed and DNI for Dahr El-Baidar is shown in Fig. 6. It is clear that wind speed and DNI

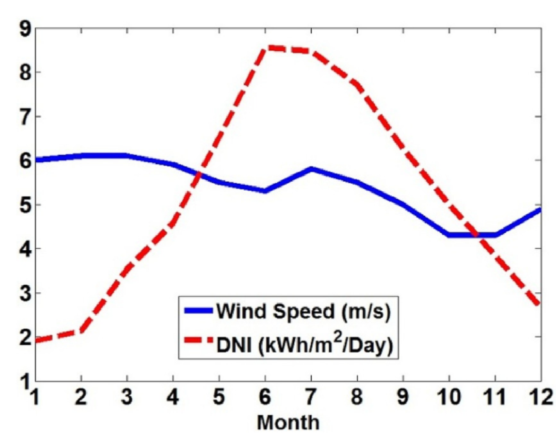

Fig. 6 – Yearly average wind speed and DNI in Dahr El-Baidar.

have opposite behaviours over the year. In winter, much more energy is available from wind while solar radiations are low. In summer, radiations have much more potential.

Fig. 7 presents the yearly AC power variation for both WT and PV. Results show that WT power is greater than the one of PV for the entire year. Despite that DNI have more potential comparing to wind speed in summer, the generated power of WT still higher because it is proportional to the cube of wind velocity. Hence, WT is recommended to be used in Dahr El-Baidar region (see Fig. 7).

The energy resulting from both systems stored in form of hydrogen using the electrolyzer. To operate this latter, the AC power of WT needs to be converted to DC using a rectifier while DC power resulting from PV can be directly used. Consequently, the useful power of WT is reduced because of the rectifier's efficiency. This is shown through hydrogen production rates presented in Fig. 8.

The energy stored in form of hydrogen is used to generate power during shortage time using the Fuel Cell system. The output power of this latter is proportional to its hydrogen consumption rate. Hence, Fuel Cell generates power profiles similar to those of hydrogen produced by the electrolyzer in case of WT and PV as shown in Fig. 9. The results also show that Fuel Cell can generate more energy from WT for nearly the entire year as expected from the results of the wind speed and DNI. With this in mind, the present case is an example of regions where wind energy has clear higher potential. Having said in other regions the difference between the obtained power using solar PV and Wind energy may not be very high and thus finding the optimal hybrid configuration may require more investigation such as an economic study.

Case study of Klaiaat Akkar

Comparison between wind speed and DNI for Klaiaat Akkar is shown in Fig. 10. It shows that wind velocity and DNI vary oppositely over the year with much more wind fluctuation comparing to the case of Dahr El-Baidar. The resulting AC powers in Fig. 11 reveal that from November to April the WT power is greater than the one of PV. For the rest of the year, PV power exceeds that of WT. Hence, in case of Klaiaat Akkar coupling between the two systems seems to be the optimal solution for weather fluctuation. Indeed, Klaiaat Akkar is a particular case with respect to the other regions as it has a potential in both solar and wind energy and thus an optimal solution should include both systems. Such case is representative for G2G systems with two green sources.

Hydrogen production rates resulting from equivalent DC powers of WT and PV are illustrated in Fig. 12. Results show

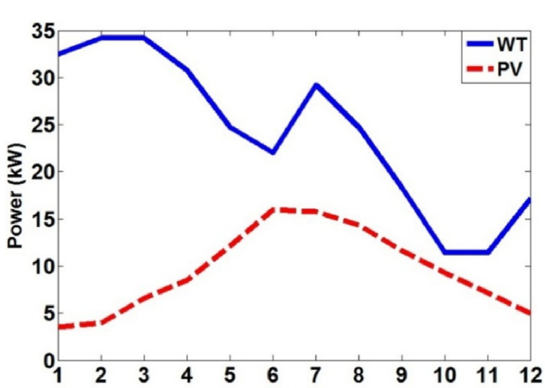

Fig. 7 – Yearly AC power variation for WT and PV in Dahr El-Baidar.

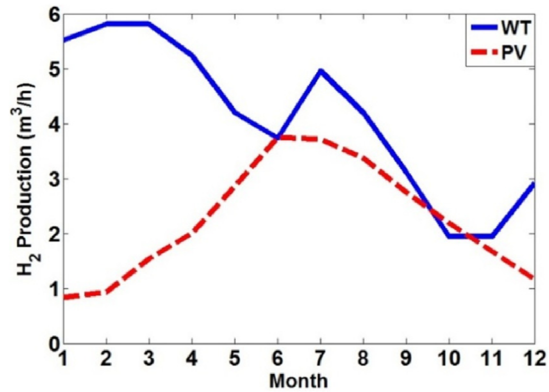

Fig. 8 – Hydrogen production rates for WT and PV in Dahr El-Baidar.

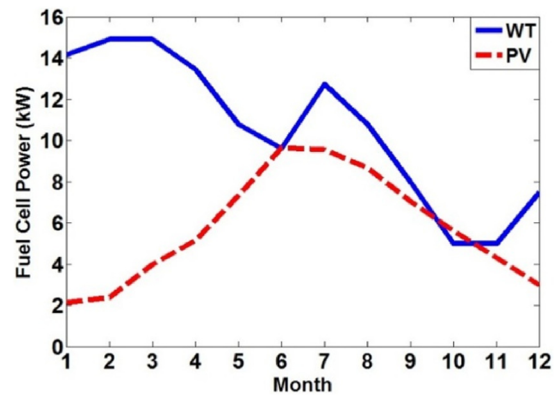

Fig. 9 – Fuel Cell output power for WT and PV in Dahr El-Baidar.

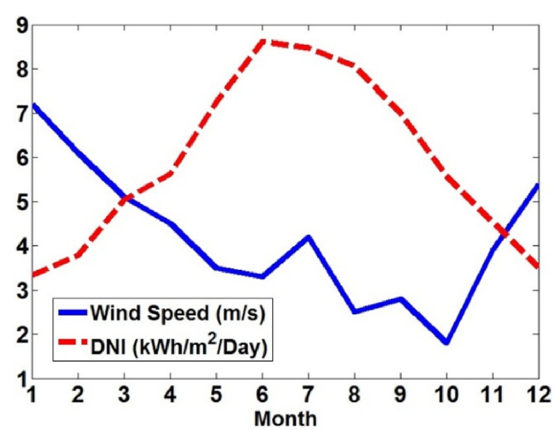

Fig. 10 – Yearly average wind speed and DNI in Klaiaat Akkar.

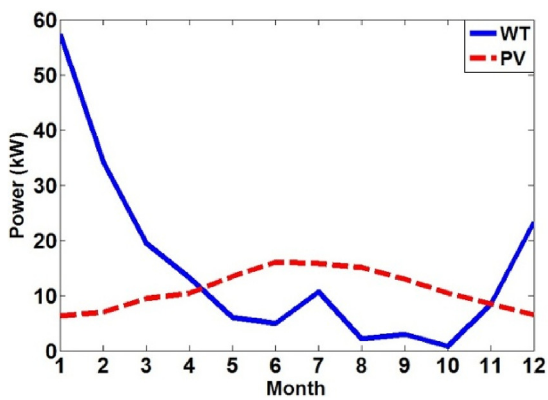

Fig. 11 – Yearly AC power variation for WT and PV in Klaiaat Akkar.

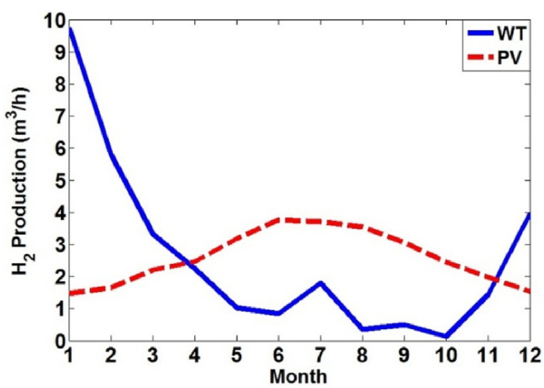

Fig. 12 – Hydrogen production rates for WT and PV in Klaiaat Akkar.

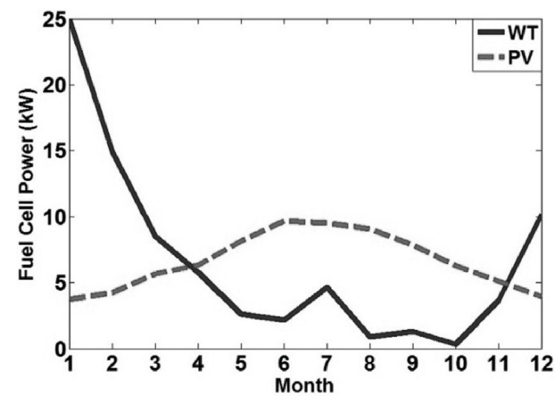

Fig. 13 – Fuel Cell output power for WT and PV in Klaiaat Akkar.

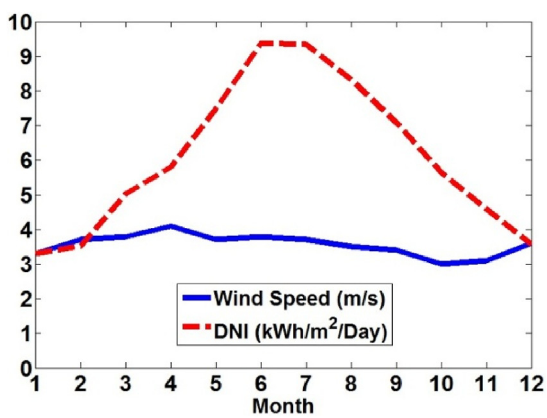

Fig. 14 – Yearly average wind speed and DNI in Rayak Bekaa.

production rates similar to power profiles. Moreover, it can be noticed that the ratio of hydrogen generation over the produced power in PV is higher comparing to WT. This is because the electrolyzer is directly connected to the PV array while in case of wind farm a rectifier is needed for AC/DC conversion. In consequence, a part of WT power is lost in the rectifier. The Fuel Cell powers arising from hydrogen storage show that much more energy can be stored from WT during the winter and from PV during the summer as shown in Fig. 13.

Case study of Rayak Bekaa

Comparison between average wind speed and DNI for Rayak Bekaa is shown in Fig. 14, where the obtained results show different behaviour of DNI and wind speed over the year. The results, show clear superiority for solar potential. This is proved through results in Fig. 15 where equivalent AC power of PV is greater than the one of WT for nearly all periods. Consequently, PV is recommended to be used in Rayak Bekaa region.

The advantage of PV over WT in Rayak Bekaa is increased when it comes to hydrogen production and Fuel Cell power generation. This is illustrated in Figs. 16 and 17. This result is due to the nature of this region that has high solar potential with relatively low wind speed. Moreover, the wind speed presents less variation and thus the obtained power from the hybrid fuel cell-wind turbine system has less fluctuation over the year with respect to the that obtained by the PV-fuel cell system.

Economical study

In this section, an economical study for hybrid PVFC and WFC is performed. It deals with the calculation of the Levelized Cost of Energy (LCOE) for both systems in the three studied locations. The LCOE represents the price of one kWh of electricity produced. It is defined as the ratio of the total life-cycle cost of the installed system over the total energy produced during the system's lifetime:

$$LCOE = \frac{Cost_{Life-Cycle}}{Energy_{Life-Cycle}} \tag{25}$$

For hybrid PVFC system:

$$LCOE_{PV/FC} = \frac{Cost_{PVArray} + Cost_{Electrolyzer} + Cost_{FC}}{Energy_{Life-Cycle\_FC}} \tag{26}$$

For hybrid WFC system:

$$LCOE_{WT/FC} = \frac{Cost_{wind\ farm} + Cost_{Rectifier} + Cost_{Electrolyzer} + Cost_{FC}}{Energy_{Life-Cycle\_FC}} \tag{27}$$

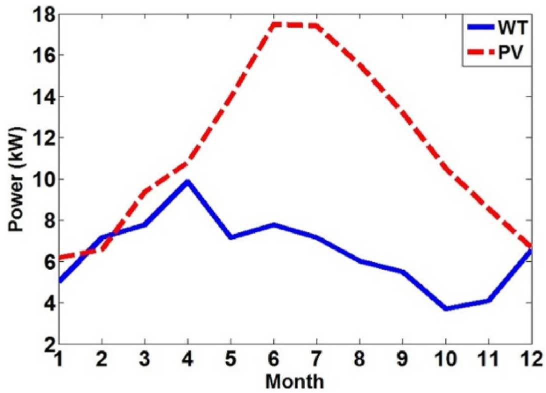

Fig. 15 – Yearly AC power variation for WT and PV in Rayak Bekaa.

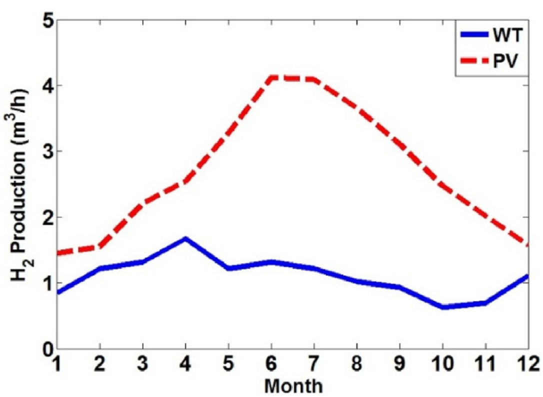

Fig. 16 – Hydrogen production rates for WT and PV in Rayak Bekaa.

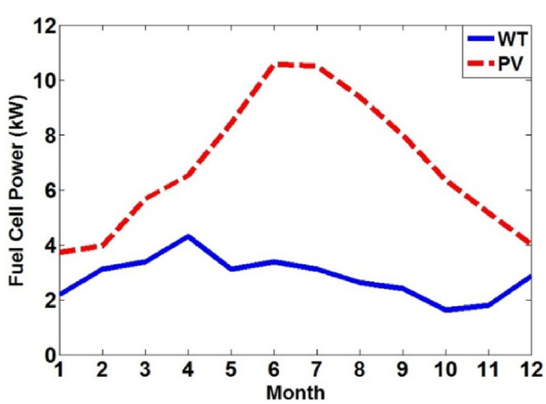

Fig. 17 – Fuel Cell output power for WT and PV in Rayak Bekaa.

The LCOE is highly affected by weather conditions (wind speed/DNI) as well as by the system's size. The former are function of the geographical location and therefore cannot be changed. The latter is mainly determined by the available land area which can be varied. The flowchart in Fig. 18 describes the proposed process for LCOE calculation based on land area.

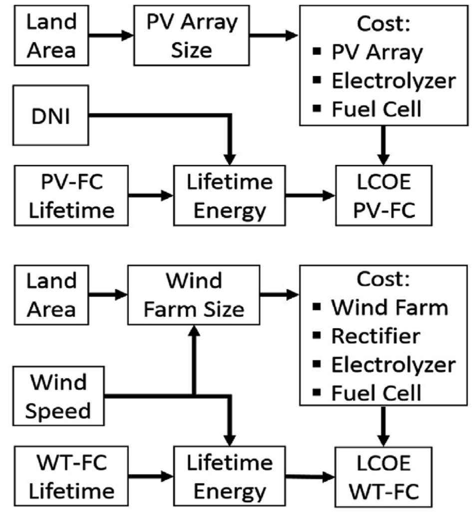

Fig. 18 – Proposed process for LCOE calculation.

Fig. 19 shows the LCOE evolution of PVFC and WFC for different areas (1000 m^2–10000 m^2) in the studied locations.

Results show that from an economic point of view the selection of the optimal system is strongly *non-linear*. In other words, there are several solutions that could be adopted depending on the imposed criterion of selection. In other terms in order to find the optimal solution, the problem should be defined by fixing one of the constraint and maximizing the output with respect to other parameters. For instance, two main constraints can be considered for this study that are the land area which is a critical parameter that varies with respect to the region and the configuration of the hybrid system that may provide different power output for different geographical location. In the frame of this study two criteria are considered, determining *optimal hybrid system for a fixed location* or determining *the optimal location for a fixed hybrid system*. To give an illustration, if the former criterion is imposed then WFC is preferred for Dahr El-Baidar and Rayak Bekaa while PVFC is generally cheaper for Klaiaat Akkar. On the other hand, if the latter criterion is fixed, then the solution is different. Indeed, in this case, the optimal solution does not depend only on the location but also on the imposed area. To

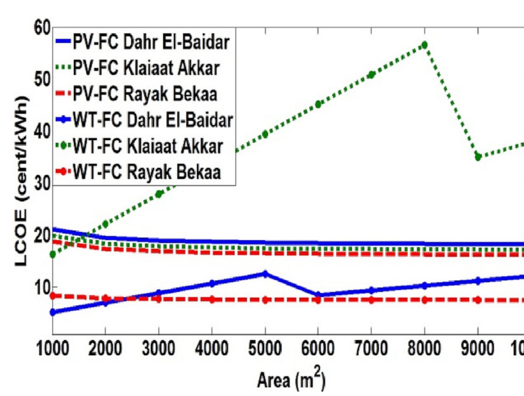

Fig. 19 – LCOE evolution of PVFC and WFC with respect to area in the studied locations.

put it another way, WFC in Dahr El-Baidar is better up to an area of 2000 m^2 whereas in Rayak Bekaa it is better for an area varying from 3000 m^2 to 10000 m^2. To understand this finding and by performing the *anatomy* of the wind map in the considered regions, it can be clearly remarked that wind speed in Rayak Bekaa is lower than that in Dahr El-Baidar. As a matter of fact, WT used in Rayak Bekaa has lower size and thus higher number of turbines can be installed within the same area with respect to the case of Dahr El-Baidar.

Conclusion

The present work proposes a Green to Green renewable energy system based on the coupling of Fuel Cell with wind turbine and PV systems through hydrogen storage. A case study covering the regions of Dahr El-Baidar, Klaiaat Akkar and Rayak Bekaa in Lebanon, is performed. The wind farm is sized according to the average wind speed, available land area, WT rotor's diameter and minimum spacing between wind turbines. The PV array sizing is based on the DNI data, the land area, the module's dimensions and the optimal tilt angle at the studied locations. The Fuel Cell and the electrolyzer are sized based on the maximum DC power produced by wind farm/PV array in the studied locations during high wind/radiation times. Mathematical models for WT, PV, Fuel Cell and Electrolyzer are elaborated. Proposed models are used to calculate the output power of each system as well as the produced quantity of hydrogen. Based on yearly wind speed and insulation data, a comparison between the three studied locations is performed. Results show that WT is recommended to be used in Dahr El-Baidar region since it produces more power for the entire year. The opposite applies in case of Rayak Bekaa region where PV is favored. Results of Klaiaat Akkar region suggest coupling between the two systems to deal with the problem of weather fluctuation over the year. Nevertheless, an economic study is carried out to evaluate the map of the optimal distribution of the different hybrid systems. Results are non-linear and reveal high dependency on the location as well as on the land area. Furthermore, the analysis is performed within two strategies. Finding *optimal hybrid system for a fixed location* or finding *the optimal location for a fixed hybrid system*. To give an illustration, for Dahr El-Baidar the optimal system is WFC whereas for Klaiaat Akkar PVFC is the best. Having said that, if the objective is to find the optimal location for a predetermined system, for WFC, Dahr El-Baidar is better up to an area of 2000 m^2. However, Rayak Bekaa is unexpectedly better if the area varies between 3000 m^2 and 10,000 m^2.

Declaration of competing interest

The authors declare that they have no known competing financial interests or personal relationships that could have appeared to influence the work reported in this paper.

REFERENCES

[1] Ozturk Merve, Dincer Ibrahim. Comparative environmental impact assessment of various fuels and solar heat for a combined cycle. Int J Hydrogen Energy 2019;44(10):5043–53. https://doi.org/10.1016/j.ijhydene.2019.01.003. ISSN 0360-3199.

[2] Kubilay Karayel G, Javani Nader, Dincer Ibrahim. Green hydrogen production potential for Turkey with solar energy. Int J Hydrogen Energy 2021;47(45):19354–64. https://doi.org/10.1016/j.ijhydene.2021.10.240.

[3] Olabi AG. The 3rd international conference on sustainable energy and environmental protection SEEP 2009 – guest Editor's Introduction. Energy 2010;35(12):4508–9.

[4] Siddiqui O, Ishaq H, Dincer I. Development and performance assessment of new solar and fuel cell-powered oxygen generators and ventilators for COVID-19 patients. Int J Hydrogen Energy 2021;46(66):33053–67. https://doi.org/10.1016/j.ijhydene.2021.07.101.

[5] Mahmoud M, Ramadan M, Naher S, Pullen K, Abdelkareem MA, Olabi A-G. A review of geothermal energy-driven hydrogen production systems. Therm Sci Eng Prog 2021;22:100854. ISSN 2451-9049.

[6] Ramadan M. A review on coupling Green sources to Green storage (G2G): case study on solar-hydrogen coupling. Int J Hydrogen Energy 2021;46(59):30547–58. https://doi.org/10.1016/j.ijhydene.2020.12.165.

[7] Kumar Khaitan Siddhartha, Raju Mandhapati. Discharge dynamics of coupled fuel cell and metal hydride hydrogen storage bed for small wind hybrid systems. Int J Hydrogen Energy February 2012;37(3):2344–52.

[8] Genç Gamze, Muhammet Çelik M, Serdar Genç. Cost analysis of wind-electrolyzer-fuel cell system for energy demand in Pınarbaşı-Kayseri. Int J Hydrogen Energy September 2012;37(17):12158–66.

[9] Ishaq H, Dincer I. Dynamic analysis of a new solar-wind energy- based cascaded system for hydrogen to ammonia. Int J Hydrogen Energy 2020;45(38):18895–911. https://doi.org/10.1016/j.ijhydene.2020.04.149.

[10] Demirdelen Tuğçe, Ekinci Fırat, Doğru Mert Başak, Karasu İlyas, Tümay Mehmet. Green touch for hydrogen production via alkaline electrolysis: the semi-flexible PV panels mounted wind turbine design, production and performance analysis. Int J Hydrogen Energy 2020;45(18):10680–95. https://doi.org/10.1016/j.ijhydene.2020.02.007.

[11] Ahmed Khouya. Levelized costs of energy and hydrogen of wind farms and concentrated photovoltaic thermal systems. A case study in Morocco. Int J Hydrogen Energy 2020;45(56):31632–50. https://doi.org/10.1016/j.ijhydene.2020.08.240.

[12] Maleki Akbar, Pourfayaz Fathollah. Sizing of stand-alone photovoltaic/wind/diesel system with battery and fuel cell storage devices by harmony search algorithm. J Energy Storage August 2015;2:30–42.

[13] Niknam Taher, Kavousi Fard Abdollah, Seifi Alireza. Distribution feeder reconfiguration considering fuel cell/wind/photovoltaic power plants. Renew Energy January 2012;37(1):213–25.

[14] Rahimi Sahand, Meratizaman Mousa, Monadizadeh Sina, Amidpour Majid. Techno-economic analysis of wind turbine – PEM (polymer electrolyte membrane) fuel cell hybrid system in standalone area. Energy 1 April 2014;67:381–96.

[15] Suha Yazici M, Ayhan Yavasoglu H, Eroglu M. A mobile off-grid platform powered with photovoltaic/wind/battery/fuelcell hybrid power systems. Int J Hydrogen Energy 30 August 2013;38(26):11639–45.
[16] Ahmad Haddad, Ramadan Mohamad, Khaled Mahmoud, Ramadan Haitham, Becherif Mohamad. Study of hybrid energy system coupling fuel cell, solar thermal system and photovoltaic cell. Int J Hydrogen Energy 2018. https://doi.org/10.1016/j.ijhydene.2018.06.0.
[17] Ahmad Haddad, Ramadan Mohamad, Khaled Mahmoud, Ramadan Haitham S, Mohamed Becherif. Triple hybrid system coupling fuel cell with wind turbine and thermal solar system. Int J Hydrogen Energy 2020;45(20):11484–91. https://doi.org/10.1016/j.ijhydene.2019.05.143.
[18] Babatunde OM, Munda JL, Hamam Y. Hybridized off-grid fuel cell/wind/solar PV/battery for energy generation in a small household: a multi-criteria perspective. Int J Hydrogen Energy 2022;47(10):6437–52. https://doi.org/10.1016/j.ijhydene.2021.12.018.
[19] Benlahbib Boualam, Bouarroudj Noureddine, Mekhilef Saad, Abdeldjalil Dahbi, Abdelkrim Thameur, Bouchafaa Farid, lakhdari Abelkader. Experimental investigation of power management and control of a PV/wind/fuel cell/battery hybrid energy system microgrid. Int J Hydrogen Energy 2020;45(53):29110–22. https://doi.org/10.1016/j.ijhydene.2020.07.251.
[20] Samy MM, Mosaad Mohamed I, Barakat S. Optimal economic study of hybrid PV-wind-fuel cell system integrated to unreliable electric utility using hybrid search optimization technique. Int J Hydrogen Energy 2021;46(20):11217–31. https://doi.org/10.1016/j.ijhydene.2020.07.258.
[21] Schnuelle Christian, Wassermann Timo, Fuhrlaender David, Zondervan Edwin. Dynamic hydrogen production from PV & wind direct electricity supply – modeling and techno-economic assessment. Int J Hydrogen Energy 2020;45(55):29938–52. https://doi.org/10.1016/j.ijhydene.2020.08.044.